

## Investigating the properties of ternary-blended self-compacting concrete with fibre

Uma Magesvari Muthaiyan<sup>1</sup> 

<sup>1</sup>Rajalakshmi Engineering College, Department of Civil Engineering, 602105, Chennai, India.

e-mail: umamagesvari.m@rajalakshmi.edu.in

### ABSTRACT

Self-Compacting Concrete (SCC) is the designation for concrete that flows under its own weight. By creating or introducing SCC, the flow ability of ordinary concrete can be enhanced. This study's primary focus is on the creation of SCC utilizing ternary blends of cementitious additives. Several tests were carried out to assess the SCC's mechanical, fresh, and durability characteristics. Energy Dispersive X-ray Analysis (EDAX) and Scanning Electron Microscope (SEM) were used to examine micro level characteristics. The mechanical and durability qualities of SCC have been improved by using a ternary blended SCC mix that contains seventy percentage of Ordinary Portland Cement, twenty percentage of Fly Ash, and ten percentage of Silica Fume. The workability of fresh concrete got reduced by increasing the fly ash, silica fume and glass fibre content that can be improved by adding super plasticizer. The strength and durability performance of hardened concrete were increases with increase in fly ash, silica fume and glass fibre in conventional concrete. The glass fiber reinforced SCC mixes with 0.4 and 0.6% of GF have a strong connection with the cement matrix, as shown by SEM pictures. As fiber dosage is increased, peak load of ternary mixed SCC increases significantly.

**Keywords:** Flyash; Silica fume; Ternary-blended SCC; Physical and durability properties.

### 1. INTRODUCTION

One of the key elements to take into account in order to give concrete strength, it need is how well it has been compacted. Concrete compaction at the site is mostly accomplished using mechanical vibrators. Not every Self-Compacting Concrete (SCC) is produced using a variety of fibers and mineral additions. The necessity for complex, tall structures has expanded due to recent improvements in the construction sector. In these situations, it becomes very difficult to guarantee full compaction of a significant amount of concrete around dense reinforcements in order to avoid voids and honeycombs, especially if compaction by human or mechanical vibrators is difficult [1]. In order to reduce aggregate waste, recycled aggregate used in concrete as a partial or full replacement for natural aggregate. Ternary blended concrete (TBC) has better strength and durability and also better for the environment. A 25-year-old building's roof slab had a recycled aggregate removed from it. The replacement of natural coarse aggregate with recycled aggregate with an increment of 0, 25, 50, 75, and 100% to create the Ternary blended SCC of grade M50. In this procedure, 10% of the cement swapped out for Metakaolin [2]. To achieve desired flow properties, Superplasticizer applied at a dose of 1.0 percent by cement weight. The L-box and V-box tests is used to assess the flow ability properties. According to the findings, natural aggregate SCC and recycled aggregate SCC have virtually equivalent compressive strengths at seven, twenty-eight and fifty-six days of concrete age [3, 4].

In these circumstances, SCC has significant flow and cohesion capabilities. The desired quality of concrete was improved by using two mineral admixtures. This study is to evaluate the axial strength and workability of SCC when added with fly ash and alccofine as mineral admixtures. For the purposes of this experiment, all concrete mixes containing different amounts of alccofine (0, 5, 10, and 15%) had a constant 30% fly ash replacement of cement. The axial strength of SCC mixes was assessed at different curing periods. Test results indicate that 10% is the best alccofine substitute. The test results demonstrate that M25 concrete may be produced by substituting fly ash and alccofine for cement [5].

SCC is a new technique that enables laborers to accomplish formwork in difficult places without segregation and without the use of external vibrations. In such settings, SCC has excellent flow and cohesiveness. In this study, two mineral admixtures were used to increase the required quality of concrete. The major purpose of this

study is to assess the axial strength and workability of SCC with mineral additives such as fly ash and alccofine. The amount of cement substituted with fly ash in this study was kept constant at 30% for all concrete mixes with different alccofine dosages (0, 5, 10, and 15%). The workability of SCC was evaluated utilizing a number of techniques. The axial strength of SCC mixes was measured at various curing periods. The best alccofine replacement, according to the results of the testing, is 10%. The results of the tests reveal that replacing cement with a mixture of fly ash and alccofine creates M25 concrete. The effect of carbon fiber on the toughness qualities of SCC. They employed fine silica fume as a supplemental cementitious material with a W/powder ratio of 0.37. Carbon fibers were added at 0, 0.5, 1.0, and 1.5% by volume of concrete. They concluded that silica fume boosted the mechanical qualities of the concrete and that the inclusion of carbon fiber enriched the strength and toughness of the concrete [6, 7]. The following characteristics of high strength concrete are shared by glass fibers (0, 0.25, 0.5, 0.75, and 1% by volume of concrete) and basalt fiber (0, 0.25, 0.5, 0.75, and 1% by volume of concrete). Fracture, compression, splitting, flexural strength, and tensile tests were performed on the notched beam. They stated that fiber insertion had no influence on the axial strength of the concrete. Basalt fiber reinforced concrete (BFRC) has better breaking tensile and flexural strengths than GFRC. The increase of more than 0.5% glass fiber had no effect on compressive strength. They concluded that basalt fiber reinforced concrete did not attain the same high fracture energy as glass fiber reinforced concrete [8]. The properties of self-compacting rubberized concrete (SCRC) and vibrated rubberized concrete (VRC) were assessed. They employed crump rubber in varied amounts by volume of sand, ranging from 0% to 50%, and they preserved the fresh characteristics while also suffering from a smaller strength loss. Mechanical characteristics including initial crack load, maximum load, ductility, and toughness decreased by increasing crump rubber. Although it didn't alter the flexural strength, applying up to 10% crump rubber improved the deformation capacity, toughness, and ductility. It concludes that it is possible to manufacture SCRC with a high percentage replacement of crump rubber percentage by 40%, while in VRC it may reach up to 50% replacement, which has the advantage of merely reducing the weight of the beams themselves and no benefit in improving the structural behavior of the beams [9].

The SCC's mechanical characteristics while using ground copper slag in place of cement. Self-Consolidated Copper Slag Concrete's mechanical and durability tests have been examined in order to confirm that the SCC's standards have been met. It suggested that replacing up to 15% of the original strength with toughened strength, and unit weights are almost similar to or slightly superior than control mixture. The difficulty in installing SCC in mat foundations and substantial wall components might result in the production of lift lines, which can cause structural problems, interlayer bond strength loss, and aesthetic flaws. In the end, they came to the conclusion that the flow of SCC over freshly cast lifts of concrete without mechanical consolidation of the preexisting material might result in the creation of lift lines with weaker bonds across the interface. Bond strength in SCC multilayer castings reduces as structural growth at the remainder of the existing SCC increases [10].

Since it performs so well, SCC has advanced the building industry. Workability, ability to flow, compressive strength, and resistance to segregation are all improved by the addition of admixtures (mineral or chemical) and other aggregate. Silica fume (SF), a mineral addition, initially improves mechanical properties while decreasing permeability. Second, the application of the chemical admixture known as the super-plasticizer (SP) to reduce water content, enhance cohesiveness, and enhance SCC passage and filling properties. On the other hand, SF can affect the physical characteristics of SCC if it is utilized excessively in cement [11]. Three fundamental criteria, including segregation resistance, passing ability, and filling ability, must be met by the SCC. The filling ability shows that the speed of the concrete flow by its own without any external force. The passing ability is an important property of SCC. The concrete can flow easily between the congested reinforcements without any segregation. SCC has to maintain its homogeneity during mixing and placing of the concrete in a structure without segregation and bleeding [12].

In place of cement, the supplemental cementitious elements are good substitute. Due of the huge cementitious content (300–600 kg/m<sup>3</sup>) and super plasticizer according to EFNARC–2005, SCC is quite expensive. Use of both natural and artificial SCMs can reduce this high cost. These SCMs' extremely small particle sizes allow the concrete's pores to be fine-tuned, which enhances the material's physical and durability capabilities [13]. A reaction between SCMs and (Ca (OH)<sub>2</sub>) that results in the production of C-S-H is started by the addition of water. In addition to increasing the concrete's mechanical, fresh, and durability qualities, the use of SCMs lowers the cost of the concrete by lowering the cement content [14]. In comparison to the regular SCC, the fly ash blended concrete exhibits reduced Cl<sup>-</sup> ion penetration over the course of a year, which has a beneficial influence on the durability attributes of SCC [15]. One of the silicon industry's waste products with a strong pozzolanic reactivity attribute is silica fume. Additionally, SF's fineness is 100 times lower than OPC's [16]. The concrete mixtures can be designed to behave almost like self-consolidating concrete. Control flow concrete has different rheological behavior when compared to CC and SCC. Flowable concrete can be enabled by suitable admixtures which work with conventional mixtures [17].

By mixing two SCMs and using them in place of some of the cement in concrete, ternary blended concrete is created. When SCMs are combined, the flaws in one SCM can be overcome by another SCM [18]. It is also feasible to include fibers into SCC mixtures without jeopardizing the concrete's self-compacting capabilities. The compressive strength of conventional concrete fell by 2.2%, 4.5%, 6.6%, 9.7%, and 11.5% after 28 days of curing when the recycled concrete aggregate (RCA) content was raised from 20% to 100% at 20% intervals. The difficulty in inserting and finishing fibrous materials in SCC mixes owing to their thixotropic nature and decreased fluidity is one of the key problems [19].

Shrinkage fissures started to appear in the early stages of concrete development, and they reduce the strength of the material. Concrete has a low tensile stress, poor impact strength, and is brittle. The fibres are included into the concrete to fix these flaws. The fibres are the minute particles of reinforcing material, and their presence helps lessen shrinkage cracks and improve the concrete's mechanical qualities [20]. SCC and FRC work together to create FRSCC. SCC with fibre reinforcement has better mechanical and durability qualities. The fibres are divided into two categories: natural and artificial fibre, depending on their size and aspect ratio. Concrete's increased durability is boosted by an alkali-resistant glass fibre that slows the spread of cracks. The ternary blended SCC lengthens the life of the structure and lowers the cost of maintenance. Fibres can be added to the ternary blended SCC to reduce the brittleness of the concrete. Additionally enhancing the concrete's tensile and impact strength is the glass fibre in SCC [21]. A process for building an SFRSCC using packing density and substituting M-sand for all river sand. The packing density-based mix design method that is suggested is simple and effective. Applying the packing density principle, the most effective mixes for 12.5mm: 20mm: M-sand were found to be 20:30:50 (maximum packing density of 68%) and 60:40 (maximum packing density of 50.5%) for Cement: GGBS [22]. Slump cone tests were utilized to optimize the dosages of fibers, whereas marsh cone research was applied to optimize the dosages of superplasticizers. In total, six combinations were created, three of which included fibers and the other three did not. Concrete mixes are produced with fiber volume fractions ranging from 0.50 to 0.750 percent by volume of concrete. Steel fiber was added to the polymer to decrease its permeability and fluidity while still meeting SCC requirements.

Use of fly ash, rice husk ash as bio waste and silica fume increases alkalinity of concrete and its performance increases the structural health performance of structure [23]. Attempts to compare and implement the flexural behavior of concrete with developed analytical model [24]. Natural fibre like sisal and nano tubes as nano composites additionally brick aggregates also have introduced to study the performance of concrete [25–28]. Addition of pine apple fibre with granite powder enhances the performance of workability and stability [29].

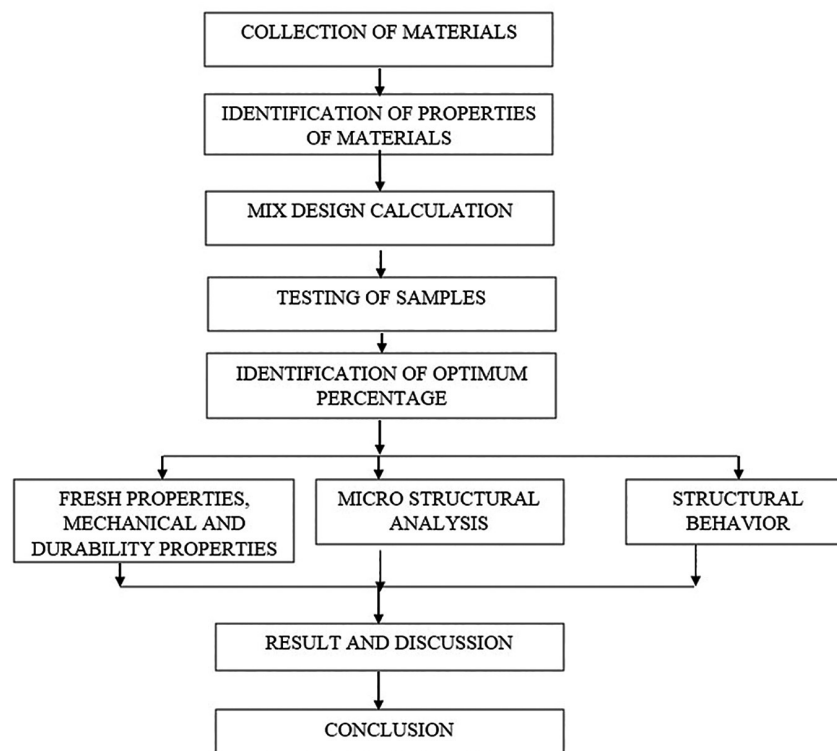


Figure 1: Methodology flowchart.

Influence of red mud and fly ash increases service life of assessment of the structural elements [30]. Analytical model was developed to assess and compare and insight the performance of real time structure interaction [31–34]. Microstructural behavior of structure was assessed and reconstructed using ct chromatography and finite element models in addition to develop machine learning model for predictive and sensitive analysis for the structural elements [35–45]. Strain rate analysis addressed the structural performance of the structural elements and its service life span of the structure [46]. There are few lacking on the SCC with fly ash silica fume and glass fibre so this research states the optimization of mix proposition with the above materials is assessed using the study of fresh, hardened and micro structural properties of concrete. The flow chart representing the methodology of work is as shown in Figure 1.

## 2. MATERIALS

### 2.1. Cement

Cement (OPC) of grade 53 was utilized in this investigation (IS 12269-2013). According to the standards in IS 12269-2013, the physical characteristics of OPC (specific gravity, consistency, start and final setting time) were assessed and shown in Table 1. Physical properties obtained values as per IS: 12269-2013 requirement relative density 3.12 – Consistency 31% – Early setting time 42 mins. Not less than 30 mins. Ultimate setting time 220 mins. Not more than six hundred mins. Chemical compositions of cement is given in Table 2.

### 2.2. Fine aggregate

The physical parameters of M-sand were evaluated in accordance with the requirements in IS: 383-2016. Fine aggregate had an average relative density of 2.62, fineness modulus of 2.6, and volumetric density of 1698 kg/m<sup>3</sup>, respectively.

### 2.3. Coarse aggregate

Crushed granite with a maximum size of 12.5 mm that complies with IS: 383-2016 was utilised as a coarse aggregate in SCC. The physical properties relative density of 2.67 (IS:383-2016), fineness modulus of 6.92 (IS:383-2016), bulk density of 1724 kg/m<sup>3</sup> (IS: 2386 (P3)-1963), aggregate impact value of 12.2% (IS: 2386 (P4)-1963) and aggregate crumble value of 21.6% (IS: 2386 (P4)-1963).

**Table 1:** Physical properties of binders.

PHYSICAL PROPERTY	CEMENT	FLY ASH	SILICA FUME
Relative density	3.12	2.12	2.62
Consistency	31%	33%	–
Early setting time	42 mins	48 mins	–
Ultimate setting time	220 mins	250 mins	–
Bulk Density (kg/m <sup>3</sup> )	1427	1134	1698
Color	Dark grey	Dark Grey	White

**Table 2:** Chemical properties of cement. Fly ash and silica fume.

CHEMICAL PROPERTY	CEMENT	FLYASH	SILICA FUME
SiO <sub>2</sub>	20.56%	58.23%	94.4%
Al <sub>2</sub> O <sub>3</sub>	5.05%	25.35%	0.62%
Fe <sub>2</sub> O <sub>3</sub>	3.15%	6.25%	0.15%
CaO	62.54%	2.67%	1.12%
MgO	2.72%	1.36%	0.72%
K <sub>2</sub> O	0.34%	0.84%	1.15%
Na <sub>2</sub> O	0.38%.	0.53%	0.22%

#### 2.4. Fly ash

In this study fly ash (class F), a by-product of coal-fired power plants. Fly ash has the following physical and chemical characteristics: Relative density of 2.12, fineness of 517 m<sup>2</sup>/kg, bulk density of 1134 kg/m<sup>3</sup>, and its physical form as powder, dark gray in color. Fly ash has the following chemical compositions: SiO<sub>2</sub> of 58.23%, Al<sub>2</sub>O<sub>3</sub> of 25.35%, Fe<sub>2</sub>O<sub>3</sub> of 6.25%, CaO of 2.67%, MgO of 1.36%, K<sub>2</sub>O of 0.84% and Na<sub>2</sub>O of 0.53%.

#### 2.5. Silica fume

Silica fume with specific gravities of 2.62 was utilized in the SCC mixtures. The physical parameters of silicafume were evaluated in accordance with the requirements in IS: 15388-2003. Chemical compositions of silica fume is given in Table 2.

#### 2.6. Chemical admixture

High range water reducing agent is utilized for making SCC which is second generation SP with the requirements according to IS 9103-1999.

#### 2.7. Glass fiber

This study employed an alkali-resistant glass fiber with a ratio of width to height 857.14, modulus of elasticity of 72000 MPa, specific gravity of 2.68, filament diameter of 14-micron, length of 12 mm.

#### 2.8. Self-compacting concrete

Concrete that self-compacts (SCC) is made with a range of fibers and mineral substances. Modern advancements in the building industry have created a need for large, intricate, multi-story constructions. To avoid voids and honeycombs, it might be challenging to guarantee that a sizable volume of concrete is completely compacted to the heavy reinforcement when compactions using human, mechanical vibrators are challenging.

### 3. MIX PROPORTION

According to the specifications of IS: 10262-2019, the SCC mix grade M30 was created. The intended mix proportions were checked against EFNARC-2005 recommendations to ensure that the necessary fluidity and resistance to segregation would be maintained. All of the mixes kept the same ratios of fly ash 20%, silica fume 10%, M-sand, coarse aggregate, and water. Through a process of trial and error, the superplasticizer dose was established to be around 2.0% of the total weight of powder in all combinations. Table 3 presents the typical SCC design mix.

Concrete cube specimens of were cast and submerged in water for three different curing ages in accordance with IS: 516–1959 specifications. The cubes were put through a compression test on a machine with a capacity of 2 tons while being loaded at a rate of 140 kN/mm<sup>2</sup> per minute. The concrete cube specimens of size 150 mm were cast and submerged in H<sub>2</sub>O for twenty-eight days. After curing, the cube specimens were takeoff from the curing tank and kept in the room temperature for twenty-four hours. Actual weight of the cube specimen was recorded before immersing in to acid solution. The acid solution was prepared with 5% of Na<sub>2</sub>SO<sub>4</sub> by volume of the water (ASTM C1012-2004). The specimens were then submerged in the acid solution for 28 to 56 days. Throughout the test time, the solution was frequently changed, and the clear space between the top of the cube specimen and it was the solution was kept above 30 mm. After 28 and 56 days of acid attack, the cube was removed and weighted. The cube specimen was tested in axial testing machine and the percentage reduction in axial strength was obtained after acid attack. The proportion between the volume of the voids and the specimen's bulk volume is used to calculate the effective porosity. The water absorption test provided these results, which were acquired. The quantity of water that the cube specimen has absorbed is indicated by the computed effective porosity. The cube specimens underwent 120 minutes of saturation before being dried at 1050°C. Based on how

**Table 3:** Design mix of SCC.

CONSTITUENT MATERIALS	DESIGN MIX VALUE
Cementitious material	514 kg/m <sup>3</sup>
Coarse aggregate	785 kg/m <sup>3</sup>
Fine aggregate	908 kg/m <sup>3</sup>
W/C	0.4

much water the specimen absorbed, the volume of voids was determined. The bulk volume is determined by the weight differential between the cube in a submerged and dry state. By removing the mortar pieces from the cube crushed during the 28-day axial strength test, the pH value of the concrete was ascertained. To acquire powder samples for pH investigation, the mortar pieces were crushed and sieved through a 150-micron sieve. To create the aqueous solution, 10 grams of mortar powder were combined with 100 ml of distilled water. To allow the alkalis in the cement paste to dissolve in H<sub>2</sub>O, the produced aqueous solution was placed in a beaker and stirred repeatedly for 72 hours. The pH probe was then inserted into the aqueous solution to determine the pH level.

## 4. RESULTS AND DISCUSSION

### 4.1. Fresh concrete properties

#### 4.1.1. Flow-ability

The slump flow value performs better than the test parameters as a qualification criterion for SCC. Table 4 displays the test results. When compared to the nominal mix, the slump value of traditional SCC is larger; as the mass of glass fibre enrich, the slump value drops.

#### 4.1.2. L-Box test

The obstruct ratio values of all ternary blended SCC mixes are presented in Table 5. When compared to the nominal mix, the obstruct ratio of traditional SCC is larger; as the amount of glass fibre enrich, the blocking ratio decreases.

#### 4.1.3. V-funnel and T5 in minutes

Results of the V-Funnel and T5 Minutes test is ternary blended SCC mixes are presented in Table 6. When compared to the nominal mix, the V funnel test and T5 mins of traditional SCC is less; as the amount of glass fibre enrich, the time increases.

**Table 4:** Values of slump flow and T500 mm.

MIX	F %	SF %	GF %	SLUMP FLOW	T500 mm SLUMP FLOW SECONDS
M1	20	10	0.0	680	3.45
M2	20	10	0.2	644	4.52
M3	20	10	0.4	612	4.79
M4	20	10	0.6	582	4.99
M5	20	10	0.8	563	5.35

**Table 5:** Values of L-box.

MIX	F %	SF %	GF %	BLOCKING RATIO (H2/H1)
M1	20	10	0.0	0.85
M2	20	10	0.2	0.81
M3	20	10	0.4	0.78
M4	20	10	0.6	0.76
M5	20	10	0.8	0.73

**Table 6:** Values of V-funnel test and V-funnel T5 minutes test.

MIX	F %	SF %	GF %	V-FUNNEL TEST VALUES (SECONDS)	T5 MINUTES TEST VALUES (SECONDS)
M1	20	10	0.0	11.5	11.6
M2	20	10	0.2	11.7	11.8
M3	20	10	0.4	11.9	12.0
M4	20	10	0.6	12.1	12.3
M5	20	10	0.8	12.3	12.7

## 4.2. Test on mechanical properties of ternary blended SCC

### 4.2.1. Axial strength

Concrete cube specimens of 15 cm in dimensions were cast and submerged in water for three different curing ages in accordance with IS: 516–1959 specifications. The cubes were put through a compression test on a machine with a capacity of 2 tons while being loaded at a rate of 140 kN/mm<sup>2</sup> per minute. In Table 7, compressive strength test results for ternary blended SCC mixes at 7, 14, and 28 days are shown. The peak strength of the mix achieves at 0.6% glass fibre with 20% fly ash and 10% silica fume.

### 4.2.2. Indirect tension

Concrete cylinder specimens of 100 dia and 300 mm high were cast and submerged in water for three different curing ages in accordance with IS: 516-1959 specifications. The cubes were put through a compression test on a machine with a capacity of 2 tons while being loaded at a rate of 140 kN/mm<sup>2</sup> per minute. In Table 8, split tensile strength test results for ternary blended SCC mixes at 7, 14, and 28 days are shown. The peak strength of the mix achieves at 0.6% glass fibre with 20% fly ash and 10% silica fume.

### 4.2.3. Modulus of rupture

Concrete beam curing ages (28 days) all in accordance with IS: 516-1959 specifications. The cubes were put through a flexural testing on a machine, while being loaded. In Table 9, modulus of rupture test results for ternary blended self-compacting concrete mixes at twenty-eight days are shown. The peak strength of the mix achieves at 0.6% glass fibre with 20% flyash and 10% silica fume.

**Table 7:** Values of axial strength.

MIX	F %	SF %	GF %	COMPRESSIVE STRENGTH (N/mm <sup>2</sup> )		
				7 DAYS	14 DAYS	28 DAYS
M1	20	10	0.0	17.64	25.32	38.78
M2	20	10	0.2	17.81	25.64	39.16
M3	20	10	0.4	18.16	26.35	40.94
M4	20	10	0.6	18.87	26.71	42.01
M5	20	10	0.8	17.81	26.35	41.65

**Table 8:** Values of indirect tension test.

MIX	F %	SF %	GF %	SPLIT TENSILE STRENGTH (N/mm <sup>2</sup> )		
				7 DAYS	14 DAYS	28 DAYS
M1	20	10	0.0	3.05	4.22	4.69
M2	20	10	0.2	3.20	4.43	4.92
M3	20	10	0.4	3.35	4.64	5.15
M4	20	10	0.6	3.42	4.73	5.26
M5	20	10	0.8	3.39	4.70	5.22

**Table 9:** Modulus of rupture results.

MIX	F %	SF %	GF %	FLEXURAL STRENGTH (N/mm <sup>2</sup> )
M1	20	10	0.0	6.8
M2	20	10	0.2	7.01
M3	20	10	0.4	7.28
M4	20	10	0.6	7.42
M5	20	10	0.8	7.31

#### 4.2.4. Modulus of elasticity

Up to 0.6% of GF, the modulus of elasticity values were increased by the inclusion of fly ash and silica fume to SCC; after that point, the values steadily decreased. The 0.6% GF mix has the highest elastic modulus value out of all the SCC mixes. In comparison to the elastic modulus of the standard (NM) SCC mix, the elastic modulus of 0.6% GF was 17.84% higher. Table 10 displays the test's outcomes for modulus of elasticity.

#### 4.3. Durability properties of ternary blended SCC

##### 4.3.1. Sulphate resistance

The concrete cube specimens of size 150 mm were cast and submerged in H<sub>2</sub>O for twenty-eight days. After curing, the cube specimens were take-off from the curing tank and kept in the room temperature for twenty-four hours. Actual weight of the cube specimen was recorded before immersing in to acid solution. The acid solution was prepared with 5% of Na<sub>2</sub>SO<sub>4</sub> by volume of the water (ASTM C1012-2004). The specimens were then submerged in the acid solution for 28 to 56 days. Throughout the test time, the solution was frequently changed, and the clear space between the top of the cube specimen and it was the solution was kept above 30 mm. After 28 and 56 days of acid attack, the cube was removed and weighted. The cube specimen was tested in axial testing machine and the percentage reduction in axial strength was obtained after acid attack. Figure 2 shows the Average loss in weight at 28 days (%)

##### 4.3.2. Salt-water resistance

The concrete cube specimens of size 150 mm were cast and submerged in water for twenty-eight days. After curing, the cube specimens were disconnected from the curing tank and kept in the room temperature for 24 hours. Actual weight of the cube specimen was recorded before immersing in to acid solution. The acid solution was prepared with 5% of sodium hydroxide (NaCl) by volume of the water. The sample were then submerged in the acid solution for 28 to 56 days. Throughout the test time, the solution was frequently changed, and the clear space between the top of the cube sample and it was the solution was kept above 30 mm. After 28 and 56 days of acid attack, the cube was removed and weighted. The cube sample was tested in compression

Table 10: Values of modulus of elasticity.

MIX	F %	SF %	GF %	MODULUS OF ELASTICITY 28 DAYS
M1	20	10	0.0	31.09
M2	20	10	0.2	31.94
M3	20	10	0.4	32.75
M4	20	10	0.6	33.31
M5	20	10	0.8	33.18

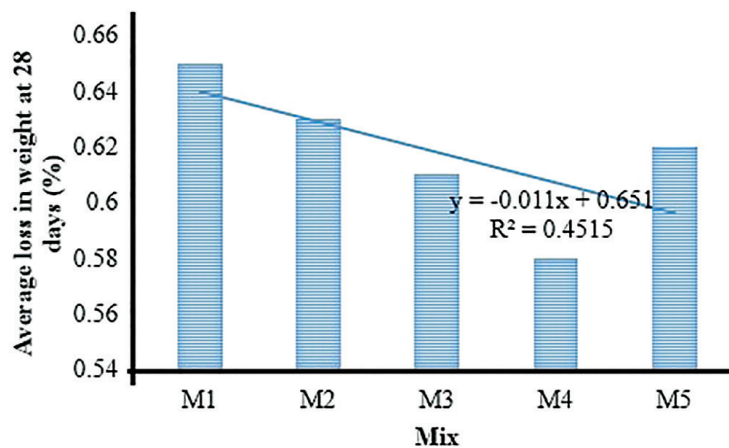


Figure 2: Average loss in weight at 28 days (%).

testing machine and percentage reduction in axial strength was obtained after acid attack. Figure 3 shows the Average loss in weight at 28 days (%).

### 4.3.3. Alkalinity

Fly ash and silica fume were added to SCC to improve the modulus of elasticity values up to 0.6% of GF; after that, the values gradually declined. Out of all the SCC mixes, the 0.6% GF mix had the greatest elastic modulus value. The elastic modulus of 0.6% GF was 17.84% more than the elastic modulus of the typical (NM) SCC mix. The results of the test for modulus of elasticity are shown in Table 8. From the results, inclusion of glass fibers in the SCC mixes slightly increases the pH values. The alkalinity test results are shown in Figure 4.

### 4.3.4. Porosity

The proportion between the volume of the voids and the specimen's bulk volume is used to calculate the effective porosity. The water absorption test provided these results, which were acquired. The quantity of water that the cube specimen has absorbed is indicated by the computed effective porosity. The cube specimens underwent 120 minutes of saturation before being dried at 105°C. Based on how much water the specimen absorbed, the volume of voids was determined. The bulk volume is determined by the weight differential between the cube in a submerged and dry state. Figure 5 displays the porosity test results.

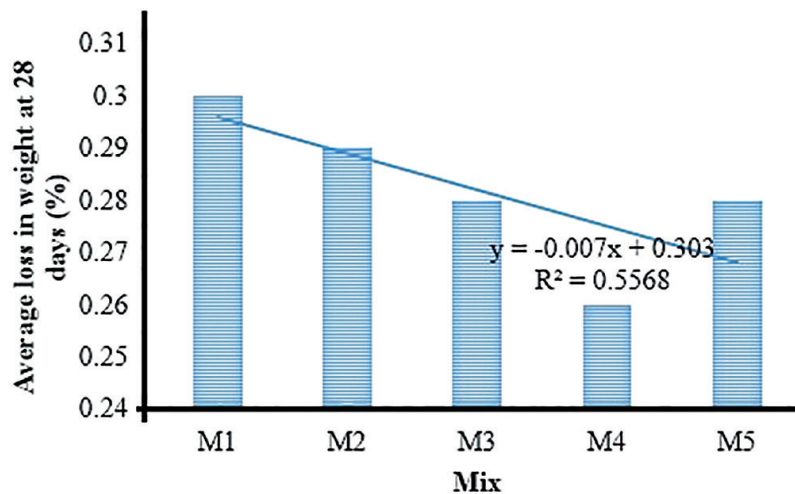


Figure 3: Average loss in weight at 28 days (%).

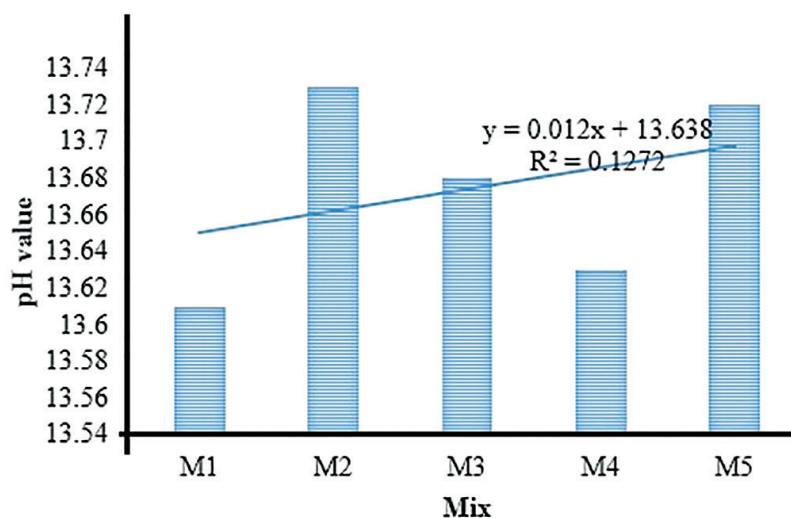


Figure 4: Alkalinity test results.

### 4.3.5. Rapid Cl- penetration test

By removing the mortar pieces from the cube crushed during the 28-day axial strength test, the pH value of the concrete was ascertained. To acquire powder samples for pH investigation, the mortar pieces were crushed and sieved through a 150-micron sieve. To create the aqueous solution, 10 grams of mortar powder were combined with 100 ml of distilled water. To allow the alkalis in the cement paste to dissolve in H<sub>2</sub>O, the produced aqueous solution was placed in a beaker and stirred repeatedly for 72 hours. The pH probe was then inserted into the aqueous solution to determine the pH level. Figure 6 shows the test results of RCPT.

### 4.4. Micro level analysis

#### 4.4.1. SEM analysis

Figures 7 and 8 depict the pictures of regular mix, M4 mix, and glass fibre reinforced SCC mixes taken using a scanning electron microscope (SEM). The M1 mix's pores have a diameter that falls between 3 and 4.25 µm, and it was discovered that the M1 mix has an uneven particle distribution and more pores. The cement matrix and aggregates have a strong connection, as seen in SEM pictures of the M4 mix. But the cement matrix had holes and fissures. When the pores' diameters were measured, they ranged from 0.95 to 2.5 µm, which is considerably less than the pores in M1 mix. The glass fibres have a strong connection with the cement matrix, as seen by the SEM images of glass fibre reinforced SCC mixes with 0.4 and 0.6% of GF. Glass fibre, a type of mineral fibre, improves the mechanical qualities of concrete to a certain extent and has a higher ability to connect with cement paste. The cement matrix held the GF firmly in place, which decreased the diameter of voids in the concrete. However, because to the reduced diameter of the glass fibre, micro fractures (less than 1 mm) developed in these mixtures.

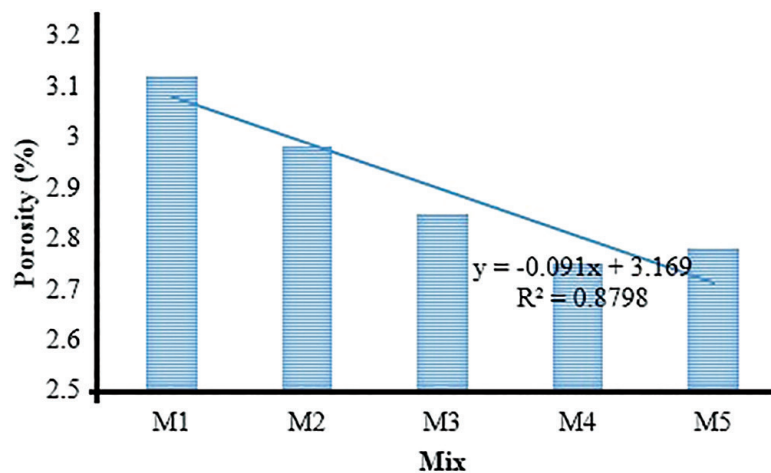


Figure 5: Porosity test results.

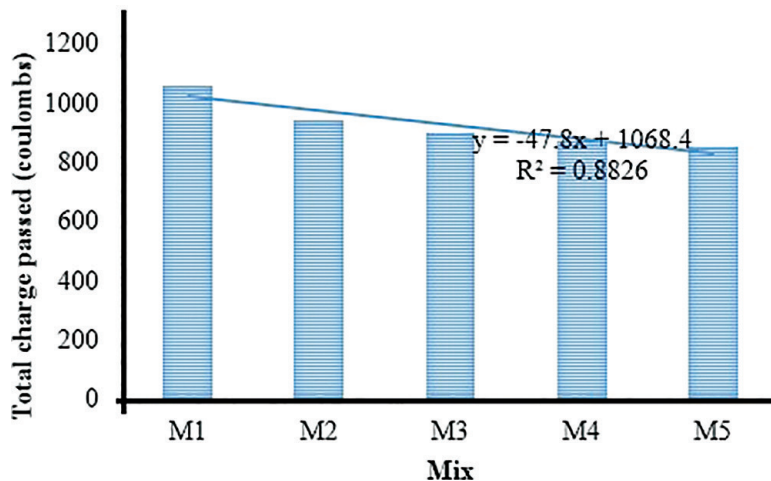


Figure 6: RCPT results of each specimen.

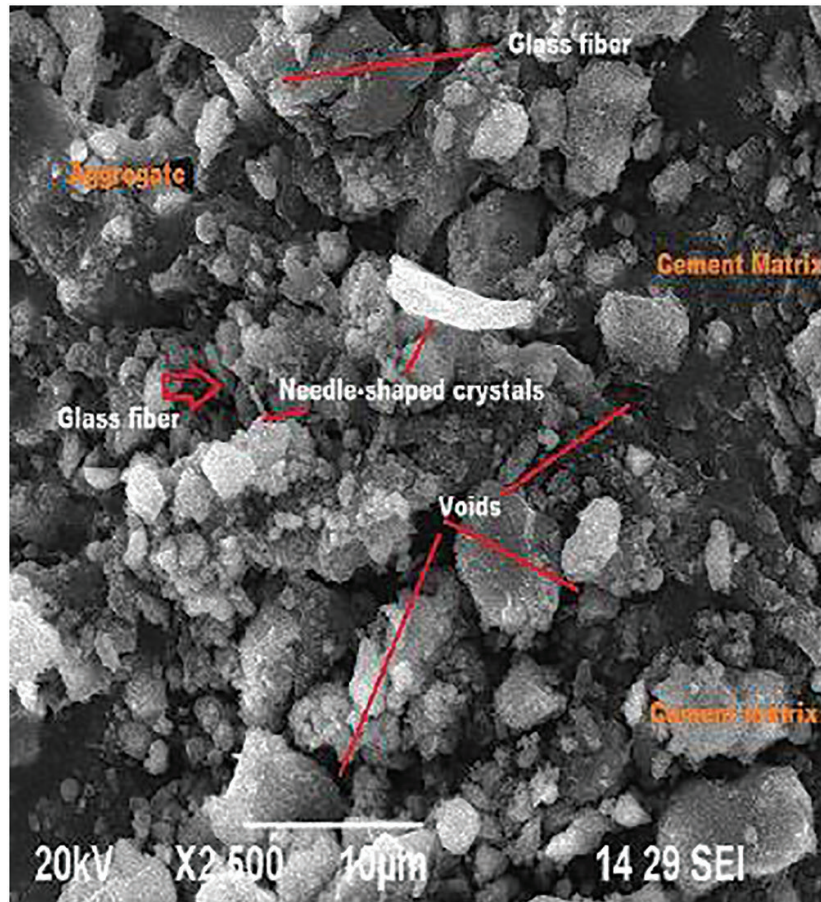


Figure 7: SEM image of M1 mix (0% of GF).

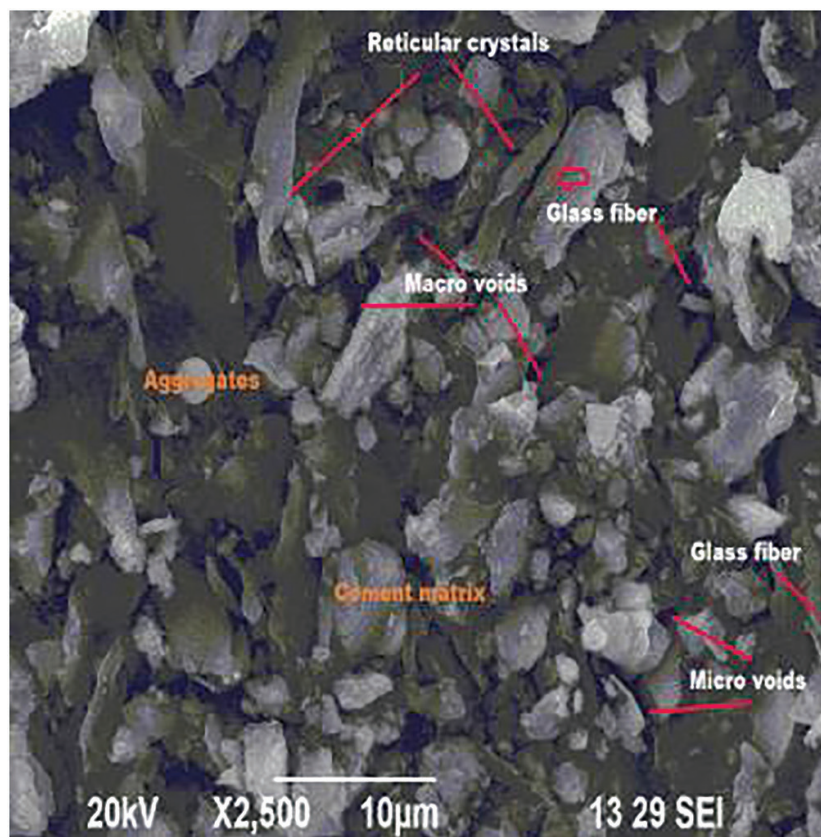


Figure 8: SEM image of M4 mix (0.6% of GF).

#### 4.4.2. EDAX analysis

The EDAX analysis of the M1 and M4 mixes is shown in Figures 9 and 10, respectively. The peak of the chemical components and their relative intensities are seen in the EDAX picture. Table 9 compares the results of the EDAX analyses of the M1 and M4 mixes. The two primary chemical elements are calcium and silica. The development of the SCC's strength is due to these two factors. The atomic weights of Ca and Si are determined using the EDAX technique.

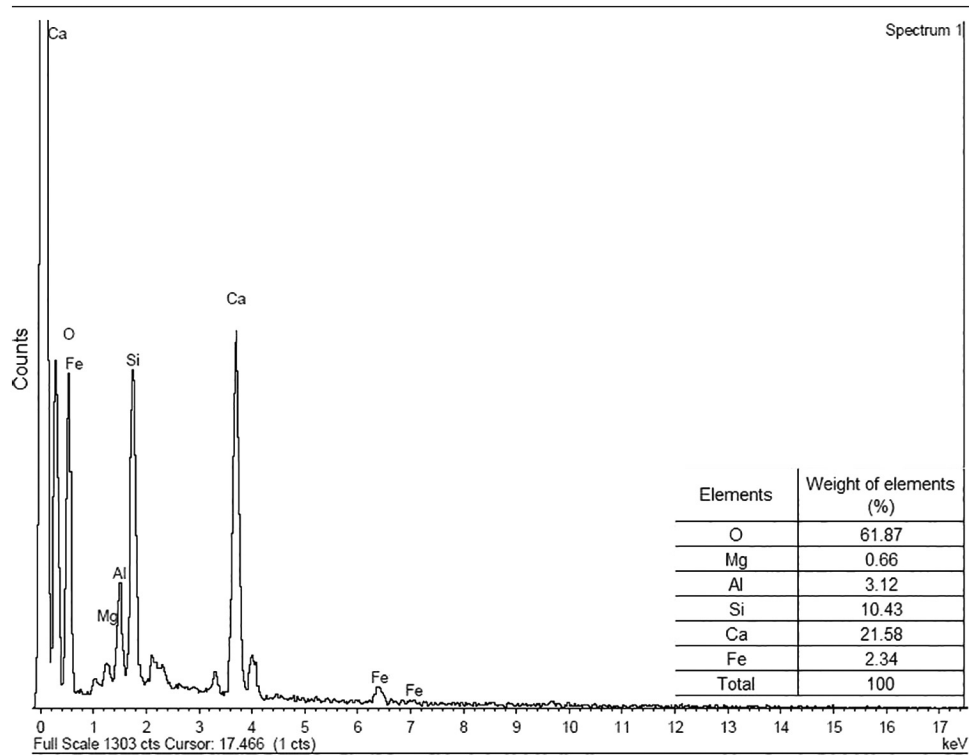


Figure 9: EDAX analysis of M1 mix.

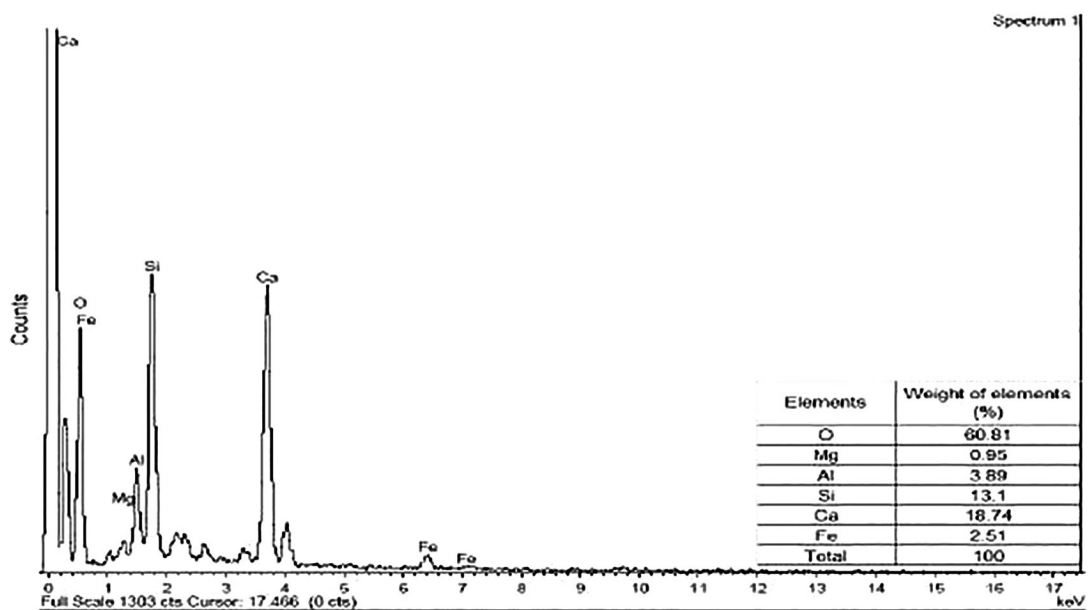


Figure 10: EDAX analysis of M4 mix.

#### 4.5. Flexural performance

##### 4.5.1. Static load test

Loading was applied through a hydraulic jack to reach 5 kN and measurements such as deflections and strains were observed at loading points and mid-point of the slab. Measurements were recorded at every 5 kN load increment. Load deflections and strain were recorded for initial crack and ultimate load. The vertical deformation at mid-span and two load points at different load levels were recorded using the deflectometeres fixed at the bottom of the slab]. The strain measurements at different load levels were recorded by a demountable mechanical strain (DEMEC) gauge with the least count of 0.001mm. Crack patterns were also marked for all loading intervals. Besides, the number of cracks developed, crack spacing and crack propagation height from the bottom of the beam were also recorded at each load interval. The load vs deflection curves and stress and strain curve are shown in Figures 11 and 12. Under vertical static load, the concrete's load-deflection curve demonstrates a sharp non-linear decrease after the first crack load and a more pronounced linear climb until a certain point. The conventionally developed slab using steel reinforcements showed ductile failure and had a respectable flexural strength.

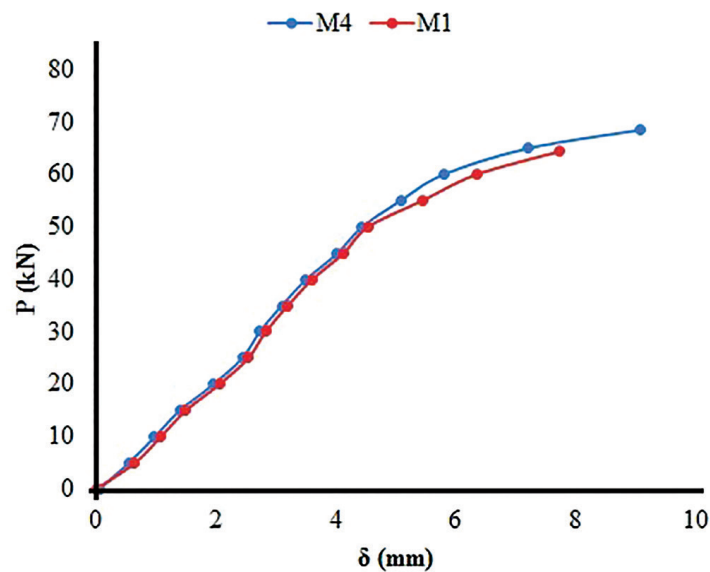


Figure 11: Load vs Deflection curve.

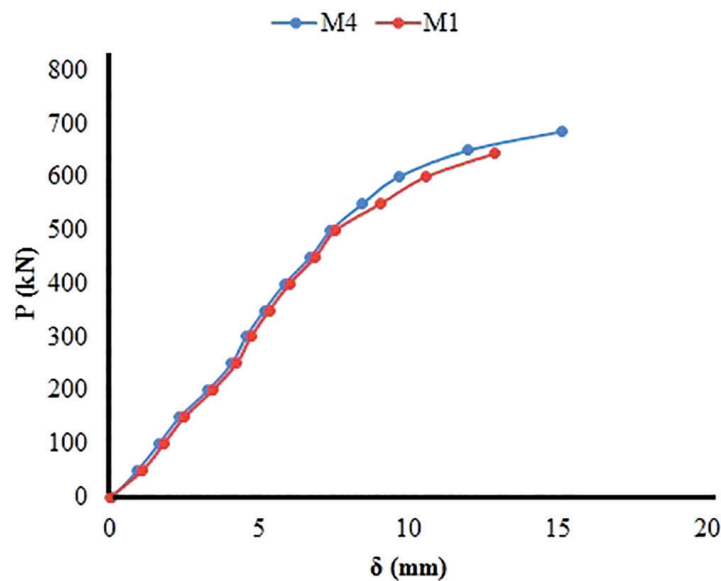


Figure 12: Stress vs Strain curve.

## 5. CONCLUSION

The conclusions presented the effects of glass fibers in the ternary blended SCC. The concrete is tested for nominal mix and controlled mix with variation in percentage of glass fibre in 0.2% and fly ash and silica fume as a fixed percentage of 20% and 10% respectively.

- The nominal mix and 20% replacement of fly ash and 10% replacement of silica fume with and without glass fibre blended concrete mixes slump values the values lie in excellent flow limit.
- With the exception of 0.8% GF replacement mixes, all ternary blended SCC mixes have a Time 500 mm slump flow time between 2 and 5 secs. The SCC's increased fibre content causes an increase in flow time.
- All ternary blended SCC mixes, with the exception of those containing 0.8% glass fibre replacement, have blocking ratios between 0.76 and 0.92. The outcome demonstrates that the SCC's high dose of glass fibre lowers the blockage ratio.
- According to EFNARC-2005, the V-funnel test results for typical SCC mixes range between 9 and 11 seconds and fall into the VF2 category. The findings indicate that an increase in glass fibre dose causes an increase in time.
- A marginal increase in the axial, split tensile, flexural strength and energy absorption was observed at early ages. The highest percentage of increase in axial strength at 28 days test was attained for 0.6% glass fibre and beyond that the strength reduces.
- The durability tests sulphate resistance and salt water resistance is much higher compared to the conventional SCC. The loss of weight in the result is much lesser. From the results, inclusion of glass fibers in the SCC mixes slightly increases the pH values.
- The diameter of pores of conventional SCC mix is in the range between 3 and 4.25  $\mu\text{m}$  and it is also found that the irregular particle distribution with more pores in the mix. SEM image of 0.6% glass fibre mix shows that good bond between cement matrix and aggregates. But small pores and cracks were observed in the cement matrix. The diameter of pores was measured and the values were in the range from 0.95 to 2.5  $\mu\text{m}$  which was comparatively smaller than the pores in conventional SCC mix.
- The moment at the first crack was more for M4 mix slab than that of recorded for M1 mix slab but the recorded deflection at corresponding loading for M1 slab was less than that of M4 slab. The ultimate moment for M1 slab was less than that of recorded for M4 slab and the recorded deflection for M1 slab was less than that of recorded for M4 slab.

## 6. BIBLIOGRAPHY

- [1] ARULSIVANANTHAM, P., GOKULAN, R., "A review on self-compacting concrete", *International Journal of Chemtech Research*, v. 10, pp. 62–68, 2018.
- [2] KRISHNA, S.S.R., VANI, V.S., BABA, S.K.V., "Studies on mechanical properties of ternary blended self compacting concrete using different percentages of recycled aggregate", *International Journal of Civil Engineering and Technology*, v. 9, pp. 1672–1680, 2018.
- [3] CELIK, K., MERAL, C., GURSEL, A.P., *et al.*, "Mechanical properties, durability, and life-cycle assessment of self-consolidating concrete mixtures made with blended portland cements containing fly ash and limestone powder", *Cement and Concrete Composites*, v. 56, pp. 59–72, 2015. doi: <http://dx.doi.org/10.1016/j.cemconcomp.2014.11.003>.
- [4] AARTHI, K., ARUNACHALAM, K., "Durability studies on fibre reinforced self-compacting concrete with sustainable wastes", *Journal of Cleaner Production*, v. 174, pp. 247–255, 2018. doi: <http://dx.doi.org/10.1016/j.jclepro.2017.10.270>.
- [5] KAVYATEJA, B.V., JAWAHAR, J.G., SASHIDHAR, C., "Investigation on ternary blended self compacting concrete using fly ash and alccofine", *International Journal of Recent Technology and Engineering*, v. 7, n. 6S, pp. 447–451, 2019.
- [6] GÜNEYISI, E., GESOĞLU, M., FAHMI, M., *et al.* "Mechanical and fracture properties of carbon fiber reinforced self-compacting concrete composites", In: *10th International Conference on Composite Science and Technology*, Lisboa, Portugal, 2015.
- [7] NAVEEN ARASU, A., NATARAJAN, M., BALASUNDARAM, N., *et al.*, "Optimization of high performance concrete composites b using nano materials", *Research on Engineering Structures and Materials*, 2023.

- [8] KIZILKANAT, A.B., KABAY, N., AKYÜNCÜ, V., *et al.*, “Mechanical properties and fracture behavior of basalt and glass fiber reinforced concrete: An experimental study”, *Construction & Building Materials*, v. 100, pp. 218–224, 2015. doi: <http://dx.doi.org/10.1016/j.conbuildmat.2015.10.006>.
- [9] DASARATHY, A.K., TAMIL SELVI, M., LEELA, D., *et al.*, “Self compacting concrete: an analysis of properties using fly ash”, *IACSIT International Journal of Engineering and Technology*, v. 7, pp. 135–139, 2018.
- [10] HU, C., LI, Z., “Property investigation of individual phases in cementitious composites containing silica fume and fly ash”, *Cement and Concrete Composites*, v. 57, pp. 17–26, 2015. doi: <http://dx.doi.org/10.1016/j.cemconcomp.2014.11.011>.
- [11] FRHAAN, W.K.M., BAKAR, H.B.A., HILAL, N., *et al.*, “Effect of silica fume and super-plasticizer on mechanical properties of self- compacting concrete: a review”, In: *3rd International Conference on Recent Innovations in Engineering (ICRIE 2020)*, pp. 01–20. 2020. doi: <http://dx.doi.org/10.1088/1757-899X/978/1/012052>.
- [12] RICARDO DE MATOS, P., FOIATO, M., PRUDENCIO JUNIOR, L.R., “Ecological, fresh state and long-term mechanical properties of high-volume fly ash high-performance self-compacting concrete”, *Construction & Building Materials*, v. 203, pp. 282–293, 2019. doi: <http://dx.doi.org/10.1016/j.conbuildmat.2019.01.074>.
- [13] SIVAKUMAR, V.R., KAVITHA, O.R., PRINCE ARULRAJ, G., *et al.*, “An experimental study on combined effects of glass fiber and metakaolin on the rheological, mechanical, and durability properties of self-compacting concrete”, *Applied Clay Science*, v. 147, pp. 123–127, 2017. doi: <http://dx.doi.org/10.1016/j.clay.2017.07.015>.
- [14] AKSHANA, V., NAVEEN ARASU, A., KARTHIGAISELVI, P., “Experimental study on concrete by partial replacement cement with silica fume”, *Journal of Critical Reviews*, v. 7, n. 17, pp. 3801–3805, 2020.
- [15] NAVEEN ARASU, N., NATARAJAN, M., BALASUNDARAM, N., *et al.*, “Utilizing recycled nanomaterials as a partial replacement for cement to create high performance concrete”, *Global NEST Journal*, v. 6, n. 25, pp. 89–92, 2023.
- [16] BHANJA, S., SENGUPTA, B., “Modified water-cement ratio law for silica fume concretes”, *Cement and Concrete Research*, v. 33, n. 3, pp. 447–450, 2003. doi: [http://dx.doi.org/10.1016/S0008-8846\(02\)00977-8](http://dx.doi.org/10.1016/S0008-8846(02)00977-8).
- [17] KUMAR, S., GURUSAMY, S., SIVAKUMAR, V., *et al.*, “Machining performance and optimization of inconel 718 using MWCNT by taguchi’s method”, *Journal of Ceramic Processing Research*, v. 23, n. 6, pp. 869–877, 2022.
- [18] SIVAKUMAR, V., VELUSAMY, P., VEERASAMY, S., *et al.*, “Comparative analysis of agro waste material solid biomass briquette for environmental sustainability”, *Advances in Materials Science and Engineering*, v. 3906256, pp. 1–7, 2022. doi: <http://dx.doi.org/10.1155/2022/3906256>.
- [19] KRISHNARAJA, R., KULANTHAIVEL, P., RAMSHANKAR, P., *et al.*, “Performance of polyvinyl alcohol and polypropylene fibers under simulated cementitious composites pore solution”, *Advances in Materials Science and Engineering*, v. 9669803, pp. 1–7, 2022. doi: <http://dx.doi.org/10.1155/2022/9669803>.
- [20] KINATTINKARA, S., ARUMUGAM, T., SAMIAPPAN, N., *et al.*, “Deriving an alternative energy using anaerobic co-digestion of water hyacinth, foodwaste and cowmanure”, *Journal of Renewable Energy and Environment*, v. 10, n. 1, pp. 19–25, 2023. doi: <http://dx.doi.org/10.30501/jree.2022.327715.1325>.
- [21] RAO, P.S., MOULI, K.C., SEKHAR, T.S., “Durability studies on glass fibre reinforced concrete”, *Journal of Civil Engineering and Science*, v. 1, pp. 37–42, 2012.
- [22] GANAPATHY, G.P., ALAGU, A., RAMACHANDRAN, S., *et al.*, “Effects of fly ash and silica fume on alkalinity, strength and planting characteristics of vegetation porous concrete”, *Journal of Materials Research and Technology*, v. 24, pp. 5347–5360, 2023. doi: <http://dx.doi.org/10.1016/j.jmrt.2023.04.029>.
- [23] THIRUKUMARAN, T., KRISHNAPRIYA, S., PRIYA, V., *et al.*, “Utilizing rice husk ash as a bio-waste material in geopolymer composites with aluminium oxide”, *Global NEST Journal*, v. 25, n. 6, pp. 119–129, 2023.
- [24] VERAPATHRAN, M., VIVEK, S., ARUNKUMAR, G.E., “Flexural behaviour of HPC beams with steel slag aggregate”, *Journal of Ceramic Processing Research*, v. 24, n. 1, pp. 89–97, 2023.
- [25] VARUTHAIYA, M., PALANISAMY, C., SIVAKUMAR, V., *et al.*, “Concrete with sisal fibered geopolymer: a behavioral study”, *Journal of Ceramic Processing Research*, v. 23, n. 6, pp. 912–919, 2022.

- [26] PALANISAMY, G., KUMARASAMY, V., “Rehabilitation of damaged RC exterior beam-column joint using various configurations of CFRP laminates subjected to cyclic excitations”, *Matéria (Rio de Janeiro)*, v. 28, n. 2, pp. no-2, 2023. doi: <http://dx.doi.org/10.1590/1517-7076-rmat-2023-0110>.
- [27] THANGAVEL, A., KUPPUSAMY, R., LAKSHMANAN, R., “Optimization of drilling parameters using GRA for polyamide 6 nanocomposites”, *Matéria (Rio de Janeiro)*, v. 28, n. 2, pp. no-2, 2023. doi: <http://dx.doi.org/10.1590/1517-7076-rmat-2022-0337>.
- [28] SOUNDAR RAJAN, M., JEGATHEESWARAN, D., “Influence of strength behavior in brick masonry prism and walette under compression”, *Matéria (Rio de Janeiro)*, v. 28, n. 1, pp. no-1, 2023. doi: <http://dx.doi.org/10.1590/1517-7076-rmat-2022-0260>.
- [29] ABISHA, Y., NALANTH, N., “Pineapple fibre as an additive to self-compacting concrete”, *Matéria (Rio de Janeiro)*, v. 28, n. 1, pp. no-1, 2023. doi: <http://dx.doi.org/10.1590/1517-7076-rmat-2022-0315>.
- [30] BAI, B., CHEN, J., BAI, F., *et al.*, “Corrosion effect of acid/alkali on cementitious red mud-fly ash materials containing heavy metal residues”, *Environmental Technology & Innovation*, v. 33, pp. 103485, 2024. doi: <http://dx.doi.org/10.1016/j.eti.2023.103485>.
- [31] LI, H., YANG, Y., WANG, X., *et al.*, “Effects of the position and chloride-induced corrosion of strand on bonding behavior between the steel strand and concrete”, *Structures*, v. 58, pp. 105500, 2023. doi: <http://dx.doi.org/10.1016/j.istruc.2023.105500>.
- [32] LIU, C., CUI, J., ZHANG, Z., *et al.*, “The role of TBM asymmetric tail-grouting on surface settlement in coarse-grained soils of urban area: Field tests and FEA modelling”, *Tunnelling and Underground Space Technology*, v. 111, pp. 103857, 2021. doi: <http://dx.doi.org/10.1016/j.tust.2021.103857>.
- [33] CAO, J., HE, H., ZHANG, Y., *et al.*, “Crack detection in ultrahigh-performance concrete using robust principal component analysis and characteristic evaluation in the frequency domain”, *Structural Health Monitoring*, pp. 14759217231178457, 2023. doi: <http://dx.doi.org/10.1177/14759217231178457>.
- [34] HE, H., SHI, J., YU, S., *et al.*, “Exploring green and efficient zero-dimensional carbon-based inhibitors for carbon steel: From performance to mechanism”, *Construction & Building Materials*, v. 411, pp. 134334, 2024. doi: <http://dx.doi.org/10.1016/j.conbuildmat.2023.134334>.
- [35] WANG, M., YANG, X., WANG, W., “Establishing a 3D aggregates database from X-ray CT scans of bulk concrete”, *Construction & Building Materials*, v. 315, pp. 125740, 2022. doi: <http://dx.doi.org/10.1016/j.conbuildmat.2021.125740>.
- [36] PANG, B., ZHENG, H., JIN, Z., *et al.*, “Inner superhydrophobic materials based on waste fly ash: microstructural morphology of microetching effects”, *Composites. Part B, Engineering*, v. 268, pp. 111089, 2024. doi: <http://dx.doi.org/10.1016/j.compositesb.2023.111089>.
- [37] CHEN, L., ZHANG, Y., CHEN, Z., *et al.*, “Biomaterials technology and policies in the building sector: a review”, *Environmental Chemistry Letters*, 2024. doi: <http://dx.doi.org/10.1007/s10311-023-01689-w>.
- [38] ZHANG, W., ZHANG, S., WEI, J., *et al.*, “Flexural behavior of SFRC-NC composite beams: An experimental and numerical analytical study”, *Structures*, v. 60, pp. 105823, 2024. doi: <http://dx.doi.org/10.1016/j.istruc.2023.105823>.
- [39] LONG, X., MAO, M., SU, T., *et al.*, “Machine learning method to predict dynamic compressive response of concrete-like material at high strain rates”, *Defence Technology*, v. 23, pp. 100–111, 2023. doi: <http://dx.doi.org/10.1016/j.dt.2022.02.003>.
- [40] HUANG, H., GUO, M., ZHANG, W., *et al.*, “Numerical investigation on the bearing capacity of RC columns strengthened by HPFL-BSP under combined loadings”, *Journal of Building Engineering*, v. 39, pp. 102266, 2021. doi: <http://dx.doi.org/10.1016/j.jobbe.2021.102266>.
- [41] HUANG, H., GUO, M., ZHANG, W., *et al.*, “Seismic behavior of strengthened rc columns under combined loadings”, *Journal of Bridge Engineering*, v. 27, n. 6, pp. 05022005, 2022. doi: [http://dx.doi.org/10.1061/\(ASCE\)BE.1943-5592.0001871](http://dx.doi.org/10.1061/(ASCE)BE.1943-5592.0001871).
- [42] ZHANG, W., KANG, S., LIN, B., *et al.*, “Mixed-mode debonding in CFRP-to-steel fiber-reinforced concrete joints”, *Journal of Composites for Construction*, v. 28, n. 1, pp. 04023069, 2024. doi: <http://dx.doi.org/10.1061/JCCOF2.CCENG-4337>.
- [43] ZHOU, C., WANG, J., SHAO, X., *et al.*, “The feasibility of using ultra-high performance concrete (UHPC) to strengthen RC beams in torsion”, *Journal of Materials Research and Technology*, v. 24, pp. 9961–9983, 2023. doi: <http://dx.doi.org/10.1016/j.jmrt.2023.05.185>.

- [44] YAO, X., LYU, X., SUN, J., *et al.*, “AI-based performance prediction for 3D-printed concrete considering anisotropy and steam curing condition”, *Construction & Building Materials*, v. 375, pp. 130898, 2023. doi: <http://dx.doi.org/10.1016/j.conbuildmat.2023.130898>.
- [45] TANG, Y., WANG, Y., WU, D., *et al.*, “Exploring temperature-resilient recycled aggregate concrete with waste rubber: An experimental and multi-objective optimization analysis”, *Reviews on Advanced Materials Science*, v. 62, n. 1, pp. 20230347, 2023. doi: <http://dx.doi.org/10.1515/rams-2023-0347>.
- [46] ZHANG, C., ABEDINI, M., “Strain rate influences on concrete and steel material behavior, state-of-the-art review”, *Archives of Computational Methods in Engineering*, v. 30, n. 7, pp. 4271–4298, 2023. doi: <http://dx.doi.org/10.1007/s11831-023-09937-6>.